In situ ellipsometric study of a palladium catalyst during the oxidation of methane

D. König [1], W.H. Weber [2], B.D. Poindexter, J.R. McBride, G.W. Graham and K. Otto

Ford Research Laboratory, Ford Motor Company, MD 3028/SRL, Dearborn, MI 48121-2053, USA

Received 28 September 1994; accepted 13 October 1994

Ellipsometry is used to follow the growth of a PdO layer on the surface of a thick Pd-film catalyst during methane oxidation at ∼ 500°C. The oxide layer that develops under rich conditions (excess CH_4) is quite porous and roughens with time. Little CO is formed during this period, but the CO_2 formation rate increases until spontaneous oscillations develop, which correlate with changes in the ellipsometric data. These changes indicate that the porous oxide rapidly converts to a metal-rich state, which has decreased catalytic activity, and then slowly reoxidizes.

Keywords: ellipsometry; methane; palladium; palladium oxide; oscillations

1. Introduction

Methane is the least reactive hydrocarbon (HC) species and thus its relative abundance in automotive exhaust gas increases as other HC's are preferentially oxidized. Methane is also especially abundant in the emissions from vehicles powered by compressed natural gas, an attractive fuel. Due to these factors and the large greenhouse effect of methane, the motivation exists to develop ways to remove methane by complete oxidation. Palladium, known as an efficient catalyst for the oxidation of methane [1], has received considerable attention, and yet its behavior is not very well understood [1–7]. Large time-dependent variations in reaction rate [2,5] and peculiar hysteretic effects [4] have prompted speculation about the oxidation state of the catalytic surface, since both Pd and PdO may be stable under typical reaction conditions [3,7–9]. The purpose of this Letter is to describe an optical technique that allows us to monitor in real time the formation

---

[1] Present address: Physikalisches Institut, J.W. Goethe-Universität Frankfurt, Robert-Mayer-Strasse 2–4, 60325 Frankfurt/Main, Germany.

[2] To whom correspondence should be addressed.

and disappearance of PdO on a thick Pd film during the catalytic oxidation of methane and to correlate changes in the activity with these changes in the catalyst surface. More detailed analyses of these experiments as well as results from measurements performed during carbon monoxide oxidation over Pd will be described elsewhere.

PdO is an ideal choice for these studies. Its optical properties have recently been measured [10], which are needed in order to interpret the ellipsometric data, and there is a strong electronic absorption peaking near ~ 500 nm (2.5 eV) that gives an easily identified spectroscopic signature. This same electronic absorption leads to a resonant Raman effect that increases the Raman strength by a factor of ~ 100 with the appropriate choice of laser frequency [11]. The resonance enhancement of the Raman signal made it possible to measure at room temperature the in situ reduction of PdO in γ-Al_2O_3 supported catalysts [12]. However, even with the resonance effect, the Raman signal is too weak in the supported catalysts at high temperature for dynamical studies. We have had some success with in situ Raman experiments using thick Pd films of the sort used here, but spectroscopic ellipsometry is more sensitive and generally gives additional useful information such as oxide film thickness and composition.

During CH_4 oxidation we find that PdO forms even under very rich conditions (excess CH_4), in which case the resulting oxide film is quite porous. The growth of this porous film greatly increases the effective surface area of the catalyst and thus leads to a large increase in the CH_4 conversion rate. Under certain conditions the film composition can spontaneously oscillate between metal rich and oxide rich, and these oscillations in the film properties are accompanied by similar oscillations in the catalytic activity.

2. Experimental

The experimental apparatus is shown schematically in fig. 1. The spectroscopic ellipsometer, manufactured by J.A. Woollam Co., is a rotating analyzer instrument [13] and is fully computer controlled. Its purpose is to measure the ellipsometric parameters Δ and ψ defined by $r_p/r_s = \tan \psi e^{i\Delta}$, where r_p and r_s are the amplitude reflection coefficients for p- and s-polarized light, respectively. For the real-time studies we record Δ and ψ at one or two wavelengths as a function of time. Spectroscopic scans are obtained over the 300–1000 nm range after the film has stabilized, either at high temperature or room temperature. Included with the instrument are extensive software capabilities for modeling the response of various multilayered structures and for determining the model parameters through linear regression analysis. Real-time ellipsometry, which has been demonstrated to have monolayer sensitivity, has been used previously in electrochemical studies and in studies of film growth and characterization in vacuum [14], but its uses in catalytic studies have been more limited [15,16].

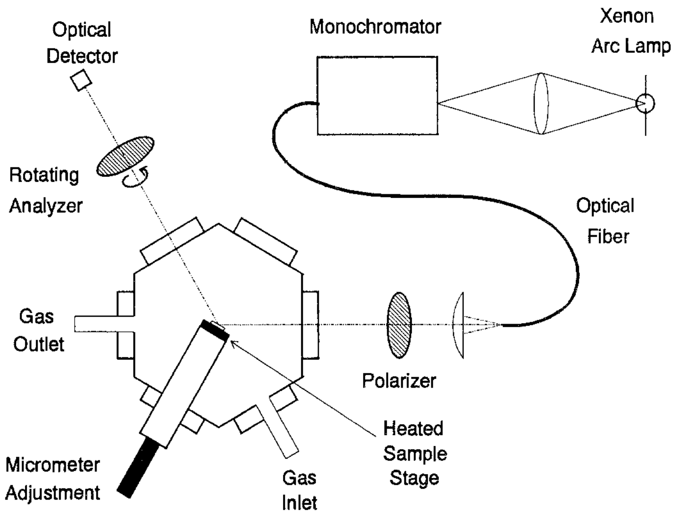

Fig. 1. Schematic drawing of the in situ spectroscopic ellipsometer apparatus.

The stainless-steel sample chamber, which was custom-made for these experiments, is hexagonal with six copper-gasketed UHV flanges: three have optical windows, two are used for the gas flows, and one has a micrometer adjustment for the sample stage and electrical feedthroughs for the heater and thermocouple leads. The heater is a pyrolytic-boron-nitride-coated disk onto which the samples are spring-mounted with a small Pt tab. The thermocouple used for temperature control is attached to the same tab, and a controller maintains its temperature to ±1 °C. The actual temperature in the region probed by the optical beam is 45° ± 10° higher, which is the value we report with the measurements to follow. This temperature was measured by a second probe thermocouple in a series of preliminary experiments. The samples are Pd films ~ 1 μm thick that have been vacuum sputtered onto $\sim 1.2 \times 1.0$ cm^2 sapphire substrates. The chamber volume is ~ 550 cm^3 and typical total flow rates are 375–750 std. cm^3/min. The feed gases are dilute mixtures of the reactants in N_2 or Ar, which are controlled with Tylan electronic mass flow controllers. In order to monitor the conversion efficiency, the exhaust gas is passed through a Beckman Instruments, model 864, infrared CO_2 sensor. In some later experiments, the gas coming out of the CO_2 sensor is then passed through an Energetics Science Inc., model 2000, CO monitor.

3. Oxide characterization

Fig. 2 shows a dynamic scan of the oxide growth on a clean Pd substrate at 440°C where we have monitored Δ and ψ as a function of time at two wavelengths, 500 and 800 nm. The 500 nm wavelength was chosen, since it is near the large peak in $\mathrm{Im}(\varepsilon)$ for PdO leading to maximum sensitivity for a small amount of PdO;

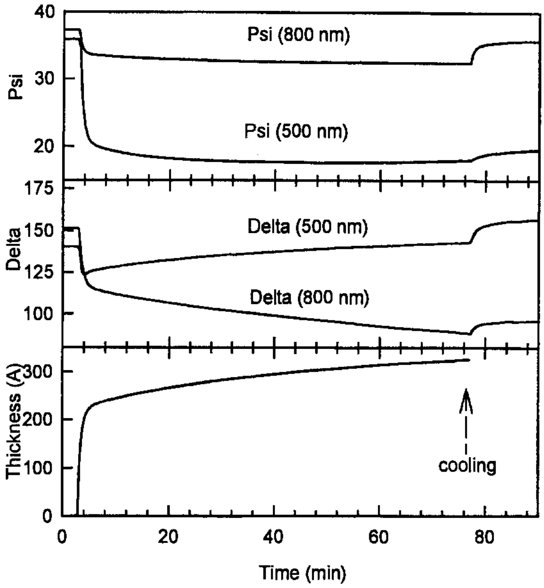

Fig. 2. Recordings of Δ and ψ at 500 and 800 nm during the growth of PdO on Pd at 440°C with 2% O_2 in N_2. The bottom panel is the film thickness determined from a subsequent model fit described in the text.

800 nm was chosen for the second wavelength, since PdO is more transparent at 800 nm, and the Δ and ψ are more sensitive to a continual change in thickness of an already thick film. The oxide growth begins at 2.5 min when 2% O_2 is added to the flow of pure N_2 and ends at 77 min when the sample is rapidly cooled to room temperature. The small changes in Δ and ψ after 77 min are due to the temperature shifts of the Pd and PdO optical properties.

Fig. 3 shows a spectroscopic scan at room temperature of the film grown in fig. 2, along with a theoretical fit. The fitting model has three adjustable parameters: the film thickness and the volume fractions of voids and Pd metal. Usually all three parameters are needed to adequately model the data. The optical properties of Pd are established by measurements on the bare film and those of PdO are known from earlier work [10]. The Bruggeman effective medium approximation [17] is used to calculate the optical properties of the composite material. Given the final thickness of the film, we determine its time dependence during growth by first fitting the high temperature film optical properties at the end of the run. These optical constants are then constrained and the film thickness is determined at earlier times by fitting the Δ and ψ variations. The result is shown in the bottom panel of fig. 2. The growth rate is similar to that observed earlier for films oxidized in air [18].

The structure observed in the spectroscopic scan of fig. 3 is an unequivocal indication of the presence of PdO. In the same wavelength region the Δ and ψ plots for Pd are smooth and featureless. The lack of perfect agreement between the

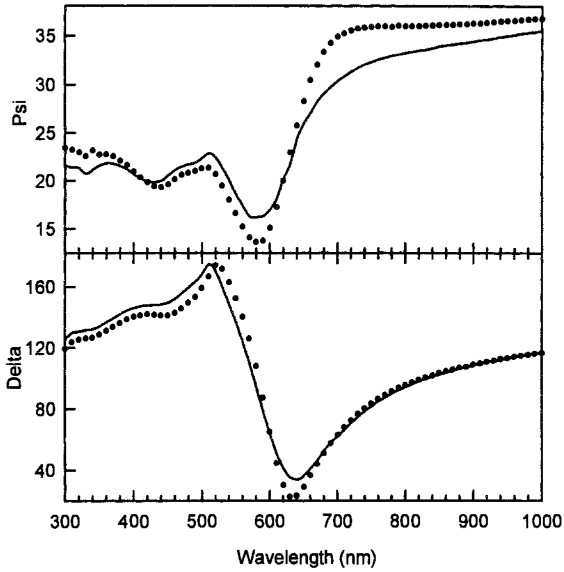

Fig. 3. Spectroscopic scan at room temperature of film grown in fig. 2 (data points) with a model fit (solid line) for an effective medium 326 Å thick composed of 84% PdO, 11% voids, and 5% Pd.

model fit and the data probably results from the film being inhomogeneous. We obtain a better fit with a two-layer model, the layer next to the metal containing mostly Pd and PdO and that on the outside containing only PdO and voids. However, the total film thickness and amount of PdO are about the same in the two models, justifying our use of the simpler one-layer fit.

4. CH_4 oxidation

Under lean conditions (excess O_2) CH_4 oxidation results in an oxide film on the Pd that is very similar to that formed without CH_4, i.e., the film is mostly PdO with a small void fraction and an even smaller Pd fraction. Under rich conditions an oxide film also forms, but the nature of the film is very different. Fig. 4 shows an example of a dynamic scan at 470°C for Pd exposed to a 375 std. cm^3/min mixture of 2% O_2 and 3% CH_4 in Ar, which is a rich mixture, since 6% O_2 would be needed to convert all the CH_4 to CO_2 and H_2O. As indicated by the large and abrupt changes in Δ and ψ immediately after the reactants are introduced at $t = 7$ min, the sample becomes completely coated with an oxide layer of a few hundred Å. Note that the conversion efficiency, as measured by the production of CO_2, is quite low at this time but continues to increase for several hours as the oxide film evolves.

In order to characterize the film during growth we interrupted the dynamic scan several times to record spectroscopic scans, which were then analyzed as in fig. 3. In each case a two-layer model was needed to obtain reasonable fits. At

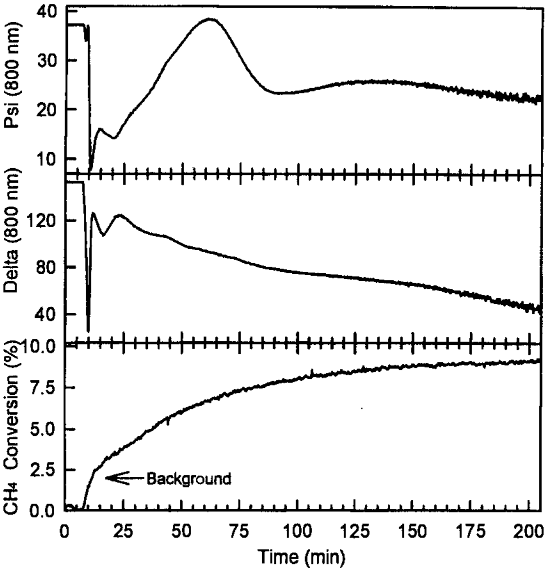

Fig. 4. Time dependence of Δ and ψ at 800 nm and the fraction of CH_4 converted to CO_2 for a Pd surface at 470°C exposed to a mixture of 3% CH_4 and 2% O_2 in Ar at $t = 7$ min. The horizontal arrow in the bottom panel indicates the CO_2 signal that does not come from the Pd catalyst, as described in the text.

$t = 16$ min the inner layer was determined to be 800 Å thick and to contain roughly equal portions of PdO, voids, and Pd, while the outer layer was 200 Å thick and was composed of 20% PdO, 80% voids, and no metal. After 45 min the inner layer was ~ 640 Å and had about the same composition as before, while the outer layer was now 770 Å thick with 16% PdO and 84% voids. Although these very high void fractions may be unrealistic, resulting from an oversimplified model, the trend is clear. As the film grows, the oxide surface becomes thicker and rougher. The increasing roughness is easily visible to the eye. The rough oxide film has a dull brown color as opposed to the lustrous greenish color of the more dense and smooth oxides. We can conclude that the slow increase in conversion efficiency in the bottom panel of fig. 4 is caused primarily by an increase in surface area of the active catalyst (PdO). The increased noise at long times in the Δ and ψ plots of fig. 4 is a result of the extreme roughness of the film. As the film roughens the specular beam becomes weaker, and ultimately one can no longer obtain reasonable ellipsometric data.

The conversion efficiency of ~ 9.0% at the end of the run in fig. 4 is limited primarily by mass transport. If all the O_2 were consumed via the conversion of CH_4 to CO_2 and H_2O, then 33% of the CH_4 would disappear. However, the diffusion length for O_2 during the residence time of the gas is 4 cm, about half the linear dimension of the chamber. Thus only about half of the O_2 actually comes in contact with the catalyst, but of this amount a large fraction is consumed.

The actual increase with time in the activity of the oxidized Pd catalyst is much larger than would be estimated by comparing the initial jump in CO_2 with the final value in fig. 4. There is a small (~ 240 ppm) shift in the zero of the infrared CO_2 sensor produced by weak CH_4 absorption lines. In addition, the cell without the Pd sample produces ~ 320 ppm under the same temperature and flow conditions, which presumably comes from the Pt tab. These two combine to yield a background signal ~ 560 ppm, which translates into 2% CH_4 conversion, as indicated by the horizontal arrow in the bottom panel of fig. 4, and accounts for most of the initial CO_2 observed. The activity above this arrow, which is attributed to the oxidized Pd surface, increases by at least a factor of 10–20 during the experiment.

Perhaps the most interesting new discovery to come out of these experiments is the observation of spontaneous oscillations in the oxidation state of the film, as evidenced by changes in the ellipsometric data, and concomitant oscillations in the catalytic activity. An example of these effects is shown in fig. 5, where the experimental conditions differ from those in fig. 4 only in the temperature, 500°C, a CH_4 concentration of 4%, and a Pd area twice as big. The oscillations started about 12 min after beginning the reaction on a fresh Pd sample. The surface before the onset of oscillations had the brownish color characteristic of the highly porous oxide. The initial changes in Δ and ψ are in the direction of a more metallic film. The peaks in Δ coincide in time with a visible change of the surface from the brown-

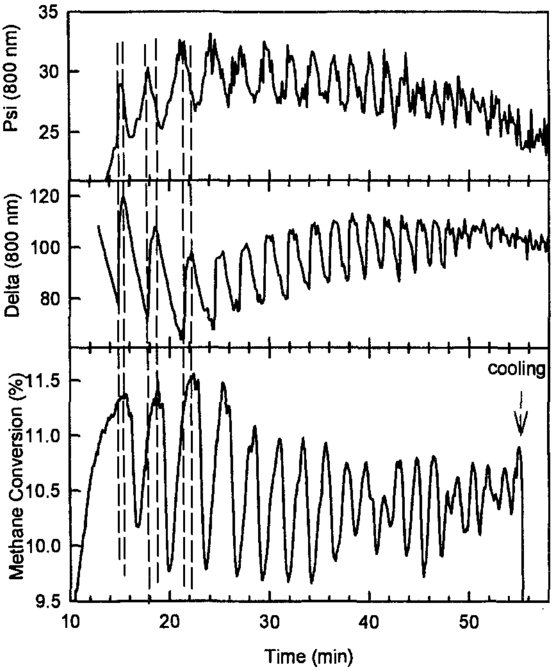

Fig. 5. Oscillations in Δ and ψ and the CO_2 production during the oxidation of CH_4 over Pd at 500°C with 4% CH_4 and 2% O_2 in Ar. Vertical lines are drawn to show the time correspondence between traces.

ish color to a gray color that nucleates at an edge and then spreads over the entire surface in a few seconds. The gray color then gradually fades to brown, and after 2–3 min the process repeats with another gray wave rapidly covering the surface. On the basis of this color change and the shifts in Δ and ψ we conclude that the porous oxide film is converting rapidly to a more metallic state and then more slowly reoxidizing. We were able to confirm this conclusion in a later experiment, in which we quenched the oscillations by rapid cooling when the sample was in the gray, metal-rich state. The surface was too rough to obtain reliable ellipsometric data, but Raman analysis showed it to be devoid of PdO. Samples in the brown state always showed a large PdO Raman signal.

The bottom panel in fig. 5 shows the signal from the CO_2 monitor. This signal is delayed ~ 1 min due to the time for mixing the gas and transporting it to the detector. Note that the peaks in Δ are followed closely by drops in the CH_4 conversion, which indicates that the more metallic surface is less active. The magnitude of the change in conversion efficiency of ~ 1–1.5% appears quite small. However, changes in CO_2 concentration at the catalyst surface are diluted by the rest of the gas in the chamber and slowed by the residence time before they are recorded downstream by the CO_2 monitor. Thus the change in catalytic activity of the surface is undoubtedly much greater than that indicated by the measured change in CO_2.

Since it is known that CO is produced when oxidizing CH_4 under rich conditions [4], we also monitored the CO in a subsequent experiment with the same temperature and gas composition as that in fig. 5. The CO concentration is unexpectedly small, typically less than 3% of CO_2, but it has an interesting time behavior. Just before the onset of oscillations, the CO_2 concentration was 4500 ppm and that for the CO too small to be measured (<5 ppm). During the first oscillation, the CO_2 dropped to 3900, while the CO abruptly *jumped* to ~ 100 ppm; both then relaxed to their original values. The rise in the CO was faster than the drop in CO_2, and the CO peak actually preceded the CO_2 minimum by 20–30 s, even though the CO monitor was downstream. These two quantities then continued to oscillate 180° out of phase with each other for the remainder of the experiment. Thus the conversion to the metal-rich state of the surface leads to increased CO generation and subsequently to decreased CO_2.

Oscillations have frequently been observed during catalytic reactions, the most often cited examples being the oxidation of CO on Pt [19,20] and on Pd [21]. A major difference here is that the chemical state of the catalyst surface changes during the oscillatory behavior, which probably explains why the oscillations we see are not perfectly periodic. The repeated oxidation and reduction of the porous film likely results in a slightly different surface morphology after each cycle. In the CO oxidation experiments on Pt and Pd only the concentrations of the reactants are involved; the chemical state of the metal surface remains unchanged. The oxidation of CH_4 on PdO is an interesting case in which the catalyst (PdO) can participate in the chemical reaction it is used to promote.

We have not fully investigated the parameter space to establish the conditions needed to obtain oscillations. However, several general comments can be made. These oscillations occurred only for rich mixtures ($[CH_4]/[O_2]$ at least 1.25) and for temperatures greater than ~ 470°C. An induction period is always required, during which a porous oxide film forms on the Pd surface. For a given temperature the oscillations occurred sooner for richer mixtures, and for a given mixture they occurred sooner for higher temperature. We have seen as many as 30 clearly defined oscillatory cycles lasting for ~ 1 h. The period usually shortens slightly with time. If the reaction is allowed to continue indefinitely, the surface always becomes so rough that it is no longer possible to obtain reliable ellipsometric data.

Although we do not claim to have a complete explanation for the oscillatory behavior, the following qualitative model offers a plausible mechanism. As the reaction proceeds, the O_2 concentration in the porous film continues to fall. If the film is rough enough and the temperature high enough, the O_2 concentration at some nucleation site will fall below that needed for the oxide to be stable. As the oxide decomposes in this highly oxygen-depleted environment, the local CH_4 reaction rate increases, and the heating produced by this exothermic reaction further drives the decomposition of PdO, the result being that the entire film is rapidly reduced. Apparently the oxide decomposition is accompanied by CO generation. The metal is now a relatively poor catalyst, which leads to a temporary drop in CO_2 production. The CO_2 concentration in the porous film builds up again, the oxide reforms, and the catalyst recovers its high activity, ready to begin another cycle.

Acknowledgement

We thank R.E. Soltis for providing the sputtered Pd films used in the experiments.

References

[1] C.F. Cullis and B.M. Willatt, J. Catal. 83 (1983) 267.
[2] T.R. Baldwin and R. Burch, Appl. Catal. 66 (1990) 359.
[3] R.F. Hicks, H. Qi, M.L. Young and R.G. Lee, J. Catal. 122 (1990) 295.
[4] S.H. Oh, P.J. Mitchell and R.M. Siewert, J. Catal. 132 (1991) 287.
[5] P. Briot and M. Primet. Appl. Catal. 68 (1991) 301.
[6] N. Mouaddib, C. Feumi-Jantou, E. Garbowski and M. Primet, Appl. Catal. A 87 (1992) 129.
[7] R.J. Farrauto, M.C. Hobson, T. Kennelly and E.M. Waterman, Appl. Catal. A 81 (1992) 227.
[8] F.H. Ribeiro, M. Chow and R.A. Dalla Betta, J. Catal. 146 (1994) 537.
[9] N.M. Rodriguez, S.G. Oh, R.A. Dalla Betta and R.T.K. Baker, in: *Proc. 6th Int. Symp. on Catalyst Deactivation,* Antwerp, October 1994, to be published.
[10] W.H. Weber, J.T. Remillard, J.R. McBride and D.E. Aspnes, Phys. Rev. B 46 (1992) 15085.
[11] J.R. McBride, K.C. Hass and W.H. Weber, Phys. Rev. B 44 (1991) 5016.
[12] K. Otto, C.P. Hubbard, W.H. Weber and G.W. Graham, Appl. Catal. B 1 (1992) 317.
[13] D.E. Aspnes and A.A. Studna, Appl. Opt. 14 (1973) 220.

[14] R.W. Collins, Rev. Sci. Instr. 61 (1990) 2029.
[15] G. Saidi and T.T. Tsotsis, Surf. Sci. 161 (1985) L 591.
[16] L.T. Tsitsopaulos and T.T. Tsotsis, Surf. Sci. 187 (1987) 165.
[17] D.A.G. Bruggeman, Ann. Phys. (Leipzig) 24 (1935) 313;
D.E. Aspnes, Thin Solid Films 89 (1982) 249.
[18] J.T. Remillard, W.H. Weber, J.R. McBride and R.E. Soltis, J. Appl. Phys. 71 (1992) 4515.
[19] F. Razón and R.A. Schmitz, Catal. Rev. 28 (1986) 89.
[20] G. Ertl, Science 254 (1991) 1750.
[21] J.E. Turner, B.C. Sales and M.B. Maple, Surf. Sci. 109 (1981) 591.